

Plastic deformation of SUS304 under in situ and post-irradiation fatigue loadings

Y. Murase ^{a,*}, Johsei Nagakawa ^{a,b}, N. Yamamoto ^a

^a National Institute for Materials Science (MEL/NIMS), 1-2-1, Sengen, Tsukuba, Ibaraki 305-0047, Japan

^b Interdisciplinary Graduate School of Engineering Sciences, Kyushu University, 6-1 Kasuga Koen, Kasuga, Fukuoka 816-8580, Japan

Abstract

Side-notched subsize specimens of SUS304 were fatigued in the unirradiated condition, during in situ irradiation with 17 MeV protons at 300 °C and post-irradiation conditions. Nano-indentation tests were conducted on the specimens fatigued for 6, 24, 100 and 200 h in the unirradiated condition, for 24 h in the in situ irradiation condition and for 200 h in the post-irradiation condition. When comparing the distribution maps of nano-hardness for the specimens fatigued for 24 h during in situ irradiation and unirradiated conditions, less significant change of hardness was detected at the notch tip for the in situ irradiation specimen. As for the post-irradiation specimen fatigued for 200 h, the area of higher nano-hardness at the notch tip was smaller than that of the unirradiated specimen fatigued for 200 h. The mechanism of the irradiation effect on fatigue behavior is discussed in terms of the plastic deformation under in situ and post-irradiation fatigue loadings.

© 2007 Elsevier B.V. All rights reserved.

1. Introduction

Structural materials for fusion and fission reactors will be simultaneously subjected to severe atomic displacement damage and external loadings. Since external loadings can include cyclic components due to thermal fluctuation and hydraulic vibration, it is important to investigate fatigue behavior under in situ irradiation in order to improve the safety design of fusion/fission reactor materials. Although available experimental data on in situ irradiation fatigue behavior are limited,

several workers [1–3] have indicated that fatigue life was substantially longer in the in situ irradiation condition than that in the post-irradiation condition. In a previous study [1], the mechanism for the irradiation effect on fatigue behavior in both in situ and post-irradiation conditions has been discussed on the basis of the interaction between radiation-induced defect (RID) clusters and moving dislocations. The general assumption is that RID clusters can act as obstacles against moving dislocations. The continuously introduced RID clusters in the in situ irradiation condition as well as the pre-injected RID clusters in the post-irradiation condition would play an important role in retarding the formation of inhomogeneous dislocation structures during fatigue loading, thereby leading to the extension of fatigue life in both irradiation conditions [1].

* Corresponding author. Tel.: +81 298 59 2552/2014; fax: +81 298 59 2014.

E-mail address: MURASE.Yoshiharu@nims.go.jp (Y. Murase).

In other studies [4,5], extensive efforts have been devoted to proving the delayed development of dislocation structures under the in situ and post-irradiation fatigue loadings. It is well known that the formation of inhomogeneous dislocation structures is closely associated with the progress of plastic strain. The present authors [4] have adopted a technique of the fracture surface topography analysis (FRASTA) to evaluate the development of plastic deformation at the crack tip by reconstructing the fatigue fracture process in both in situ and post-irradiation conditions. The results of FRASTA have suggested that the development of plastic deformation at the crack tip was more significantly delayed in the in situ than that in the post-irradiation condition. However, in this technique, the plastic deformation in the fatigue process prior to crack propagation could not be examined. A significant irradiation effect on the process of crack initiation has been implied from the results of striation analysis performed in the previous study [1].

The techniques of indentation hardness measurements such as Vickers microhardness [6,7] and nano-hardness [8] measurements have also been utilized to analyze the development of plastic deformation at the crack tip during fatigue loading. Their application to the assessment of fatigue behavior is based on the assumption that the progress of plastic strain can be reflected in the measured hardness. Although microhardness measurements could be beneficial to detect a larger plastic zone at the crack tip in the crack propagation process, the nano-indentation technique would be suitable to examine the smaller plastic zone with higher resolution of hardness in the crack initiation process. In the present study, plastic deformation of SUS304 in the crack-starter notch under in situ and post-irradiation fatigue loadings was examined using the nano-indentation technique. The objective of the present work is to demonstrate the mechanism of the irradiation effect on fatigue behavior in both in situ and post-irradiation conditions in the fatigue process prior to crack propagation.

2. Experimental procedure

The material used in the present study was a commercial SUS304 stainless steel with chemical composition of 18.2Cr–8.4Ni–0.06C–0.46Si–0.031P–0.007S–1.23Mn–balance Fe. Specimens were punched from the cold-worked sheet of 0.15 mm in thickness in the shape shown in Fig. 1.

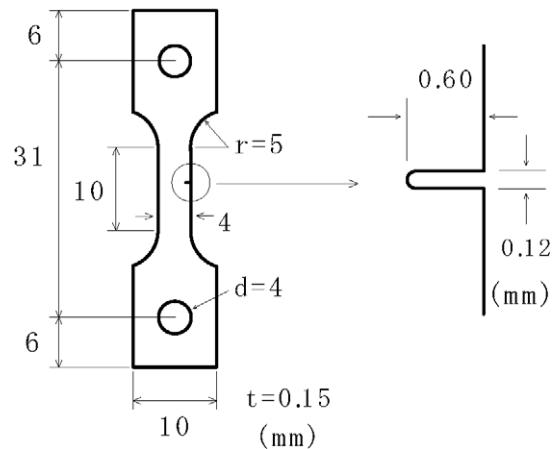


Fig. 1. Dimensions of specimen for fatigue tests.

The specimen size was $4 \times 10 \times 0.15$ mm in gauge, and a crack-starter notch was introduced by spark erosion from the edge of the gauge to 0.60 mm in depth and 0.12 mm in width. Final heat treatment at 925 °C for 30 min yielded a single-phase of austenitic structure with average grain size of 12 μm . The fatigue loading mode was tension–tension in load control with a maximum stress of 122.4 MPa and a minimum stress of 24.5 MPa under a constant loading rate of 50 MPa/s. The maximum stress is 90% of the yield stress at the notched ligament at 300 °C. In the present 17 MeV proton irradiation, atomic displacement rate was adjusted to 1×10^{-7} dpa/s with an error range of $\pm 11\%$. The specimen was cooled with circulating helium gas in order to compensate the beam heating. The specimen temperature was controlled at 300 ± 3 °C by adjusting the output of helium gas heater during the in-beam, post-irradiation and unirradiated fatigue tests as well as during the pre-irradiation for the post-irradiation tests. The details of temperature control system, irradiation condition and the in-beam fatigue experimental setup were described elsewhere [1,9].

Fatigue tests were conducted for 6, 24, 100 and 200 h in the unirradiated condition. A fatigue time of 200 h corresponded to half of the fatigue lifetime (400 h) in the unirradiated condition. Fatigue tests were also performed for 24 h during the in situ irradiation as well as for 200 h after irradiation for 24 h (0.00864 dpa). After the fatigue tests, optical microscope (OM) observation was performed for all specimens. Although some severe trails of fatigue damage were observed at the notch tip for the specimen fatigued for 200 h in the unirradiated

condition, no fatigue crack formed at the notch tip was detected for all specimens. All the fatigued specimens were then electrochemically polished to obtain flat surface for the nano-indentation tests. During the polishing, the surface and side-edge of 'as-fatigued' specimen was removed to 10 μm in depth and 50 μm in length, respectively. The nano-indentation tests were conducted on the electrochemically polished surface using a nano-indentation device (Elionix, ENT-1100) at room temperature. A triangular pyramidal diamond indenter (Berkovich indenter) with a 65° semiapex angle was employed in this device. Fig. 2 shows the OM photo of electrochemically polished surface for the specimen fatigued for 100 h in the unirradiated condition. The measured points were arranged in a mesh pattern with 25 μm apart in the area of 250 \times 250 μm at 60 μm away from the notch tip of 'as-fatigued' specimen (see Fig. 2) in order to describe a distribution map of nano-hardness for all specimens. At each measured point, the indentation load was applied with a constant loading speed of 1.96 mN/s, held at 9.8 mN for 1 s and then removed. During the loading/unloading process in the indentation test, the load was monitored along with the displacement with a resolution of 3.92 nN and 0.3 nm, respectively. When the loading/unloading profile was distorted, the measurement was re-conducted at an alternate point which was 10 μm away from the previous measured point (see Fig. 2). The nano-hardness, H , is defined as

$$H = P/A(h_c), \quad (1)$$

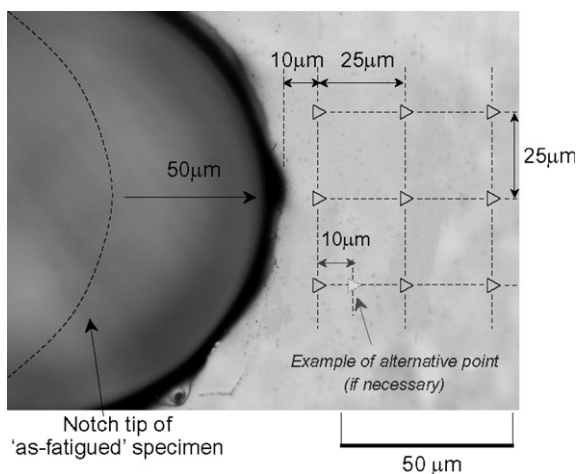


Fig. 2. Arrangement of the measured points for nano-indentation test on the electrochemically polished specimen.

where P is the indentation load (9.8 mN) and A , as a function of contact depth (h_c), is the projected area of contact between the indenter and the specimen surface. In the present study, a geometric relationship between A and h_c was adopted as follows:

$$A(h_c) = 3^{3/2} \times \tan^2 65^\circ / \sin 65^\circ \times h_c^2. \quad (2)$$

A typical nano-hardness calculated from Eqs. (1) and (2) was 2.5 GPa for the specimen without irradiation and fatigue damage. Besides the fatigue and nano-indentation tests, tensile tests were also performed for the specimens without a side-notch in both post-irradiation (0.00864 dpa) and unirradiated conditions at 300 °C. The stress–strain curves were examined in terms of the relationship between flow stress and plastic strain for both specimens.

3. Results and discussion

The stress–strain curves from the tensile tests for the irradiated (0.00864 dpa) and unirradiated specimens were shown in Fig. 3. Increases of 0.2% yield stress (0.2% YS) and ultimate tensile strength (UTS) as well as the decrease of elongation is shown for the irradiated specimen. These changes in tensile properties imply the irradiation hardening at the dose level of 0.00864 dpa. Irrespective of the changes in tensile properties, the stress–strain curves for both specimens indicated similar work hardening behavior. Fig. 4 presents the distribution maps of nano-hardness with OM photos taken at the

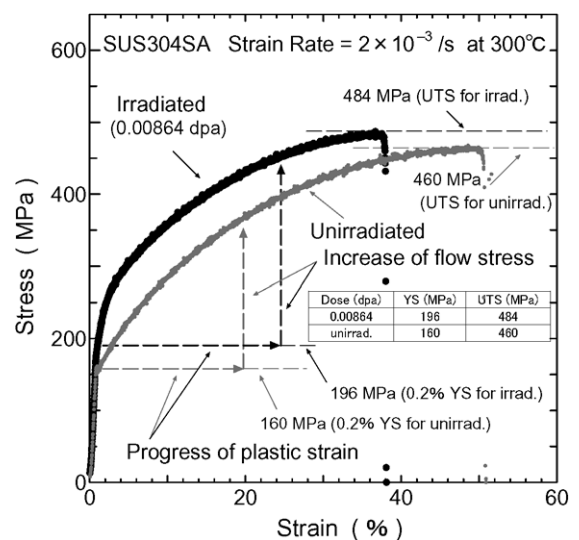


Fig. 3. Stress–strain curves for the irradiation (0.00864 dpa) and unirradiated specimens without side-notch tested at 300 °C.

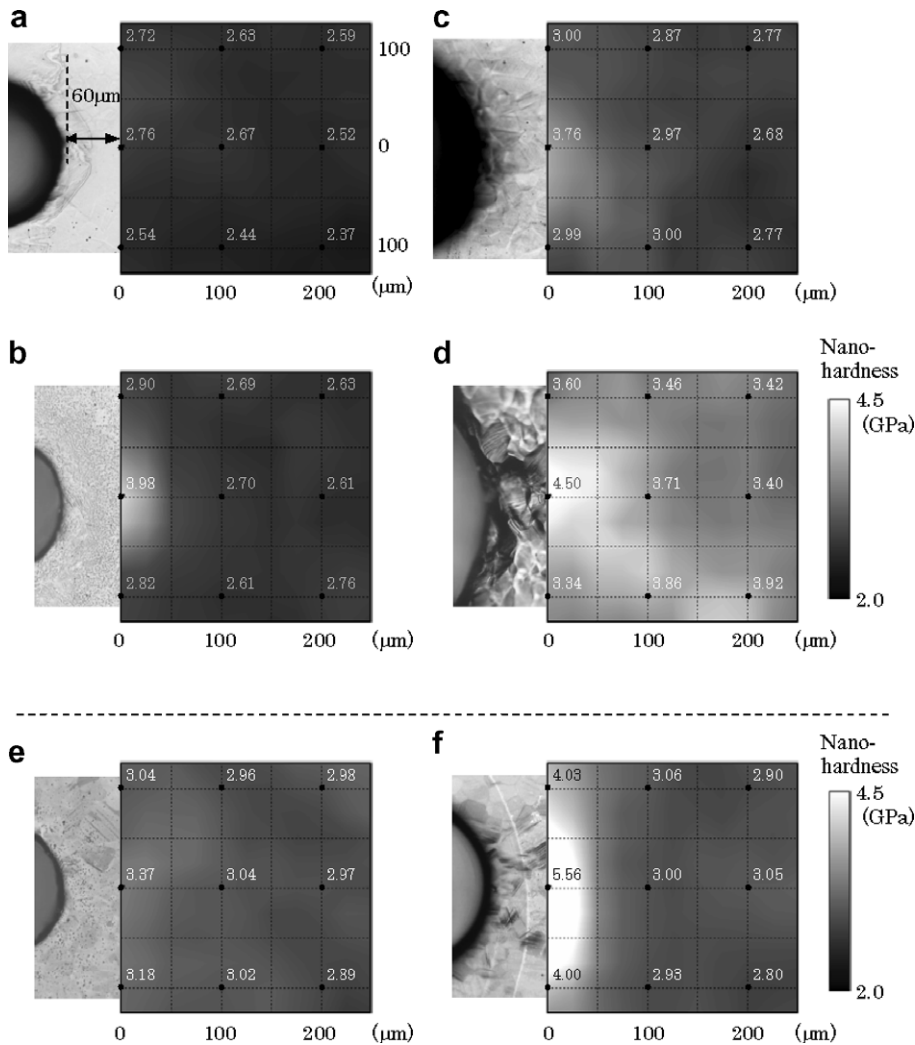


Fig. 4. Distribution maps of nano-indentation hardness with OM photos of 'as-fatigued' specimens at the crack tip fatigued for (a) 6 h, (b) 24 h, (c) 100 h and (d) 200 h in the unirradiated condition, (e) 24 h in the in situ irradiation condition and (f) 200 h in the post-irradiation condition. The values of nano-hardness (GPa) are shown at several points in these maps.

notch tip of the specimens fatigued for 6, 24, 100 and 200 h in the unirradiated condition, 24 h in the in situ irradiation condition and 200 h in the post-irradiation condition. The distribution map is displayed with black–white gradation ranging from 2.0 (black) to 4.5 GPa (white) of nano-hardness. In the unirradiated specimens shown in Fig. 4(a)–(d), the area of higher hardness appeared at the notch tip and then extended with increase of fatigue time. In comparison with the specimens fatigued for 24 h between in situ and unirradiated conditions (see Fig. 4(e) and (b)), the change of hardness was less significant at the notch tip while the hardness was slightly higher in all the measured area except the

notch tip for the in situ irradiation specimen. As for the specimen fatigued for 200 h in the post-irradiation condition (Fig. 4(f)), the area of higher hardness at the notch tip was smaller than that for the unirradiated specimen (Fig. 4(d)).

It is well accepted that the indentation hardness is closely associated with other common mechanical properties. In particular, reasonable proportionality between changes in Vickers microhardness and yield stress has been reported for various steels [10]. Since good agreement of Vickers microhardness with nano-hardness has been addressed in the range of nano-hardness from 0.7 to 3 GPa [11], a linear relationship between changes in nano-hardness and

yield stress could be also feasible for various alloys in many cases. In the present study, the measured nano-hardness for the specimen without irradiation and fatigue damage was about 2.5 GPa, within the range of 0.7–3 GPa. Furthermore, stress–strain curves shown in Fig. 3 indicated the increase of flow stress with the progress of plastic strain for both irradiated and unirradiated specimens. Therefore, it is reasonable that the development of plastic deformation can be correlated with the increase of nano-hardness in the present study. A series of distribution maps of nano-hardness for the unirradiated specimens shown in Fig. 4(a)–(d) successfully demonstrated the expansion of plastic zone with the increase of fatigue time. As for the in situ irradiation specimen (Fig. 4(e)), a slightly higher hardness in all the measured area except the notch tip than that for the respective unirradiated specimen (Fig. 4(b)) would reflect the irradiation hardening. Less significant change of hardness at the notch tip for the in situ irradiation specimen shown in Fig. 4(e) strongly suggests the delay in the development of plastic deformation in the in situ irradiation condition. Retarded development of plastic deformation would be also implied in the post-irradiation condition, because the area of higher hardness at the notch tip was smaller for the post-irradiation specimen (Fig. 4(f)) than that for the respective unirradiated specimen (Fig. 4(d)). Thus, the present results of nano-indentation tests provide reliable evidence for the delay in the development of plastic deformation even in the fatigue process prior to crack propagation in both in situ and post-irradiation conditions. Since the formation of inhomogeneous dislocation structures is closely associated with the progress of plastic strain, the delay in the development of plastic deformation inferred in the present results strongly supports that the interaction between RID clusters and moving dislocations would be an influential mechanism for the irradiation effect on fatigue behavior in both in situ and post-irradiation conditions.

Application of the nano-indentation technique to the assessment of fatigue behavior may be effective, but it needs special care because of the various factors influencing the treatment of specimen surface and the experimental environment [12]. The measured nano-hardness of 2.5 GPa for the specimen without irradiation and fatigue damage in the present experiment appeared to be higher than the usual Vickers microhardness (~ 2.0 GPa) measured for solution-annealed austenitic stainless steels. This

deviation of nano-hardness may be attributed to the subtle vibrations from other instruments installed in the laboratory [12]. However in case of an upper shift of nano-hardness, the measured distribution map should be meaningful to indicate the development of plastic deformation when the hardness data obtained from the distorted loading/unloading profiles were eliminated to keep the scattering of hardness lower in the distribution map. The usefulness of nano-indentation technique for the assessment of irradiation effect on fatigue behavior was also demonstrated in the present study.

4. Conclusions

Side-notched subsize specimens of SUS304 were fatigued in the unirradiated condition, during in situ irradiation with 17 MeV protons at 300 °C and post-irradiation conditions. Nano-indentation tests were conducted on the specimens fatigued for 6, 24, 100 and 200 h in the unirradiated condition, the specimen fatigued for 24 h in the in situ irradiation condition and fatigued for 200 h in the post-irradiation condition. The distribution map of nano-hardness at the notch tip demonstrated expansion of the plastic zone with increase of fatigue time in the unirradiated condition. As for both in situ and post-irradiation specimens, delayed development of plastic deformation at the notch tip was implied in their distribution maps compared with those for the respective unirradiated specimens. Since the formation of inhomogeneous dislocation structures is closely associated with the progress of plastic strain, the delay in the development of plastic deformation inferred in the present results strongly supports that the interaction between radiation-induced defect clusters and moving dislocations would be an influential mechanism for the irradiation effects on fatigue behavior in both in situ and post-irradiation conditions. The usefulness of nano-indentation tests for the assessment of the irradiation effect on fatigue behavior was also demonstrated in the present paper.

Acknowledgement

This work was financially supported by the Budget for Nuclear Research of the Ministry of Education, Culture, Sports, Science and Technology, based on the screening and counseling by the Atomic Energy Commission.

References

- [1] Y. Murase, Johsei Nagakawa, N. Yamamoto, J. Nucl. Mater. 302 (2002) 211.
- [2] R. Scholz, J. Nucl. Mater. 212–215 (1994) 546.
- [3] H. Mizubayashi, S. Okuda, K. Nakagome, H. Shibuki, S. Seki, Mater. Trans. Japan Inst. Metals 25 (1984) 257.
- [4] Y. Murase, Johsei Nagakawa, N. Yamamoto, J. Nucl. Mater. 322 (2003) 249.
- [5] Y. Murase, J. Nagakawa, N. Yamamoto, ASTM STP 1418 West Conshohocken, 2002, 211.
- [6] D. Ye, Z. Wang, Int. J. Fatigue 23 (2001) 85.
- [7] W. Maeng, M. Kim, J. Nucl. Mater. 282 (2000) 32.
- [8] M. Nystrom, E. Soderlund, B. Karlsson, Int. J. Fatigue 17 (1995) 141.
- [9] Y. Murase, J. Nagakawa, N. Yamamoto, Y. Fukuzawa, ASTM STP 1366 ASTM, West Conshohocken, 2000, 713.
- [10] G.E. Lucas, G.R. Odette, R. Maiti, J.W. Sheckherd, ASTM STP 956 ASTM, Philadelphia, 1987, 379.
- [11] P.M. Rice, R.E. Stoller, Proc. Mater. Res. Soc. Symp. 649 (2001) Q7.11.1.
- [12] Japanese Industrial Standard, Method for Ultra-low Loaded Hardness Test, JIS Z 2255, 2003.